

Magnetism based on nitrate-nitrate interactions: The cases of LiNO_3 , $\text{K}_{0.5}\text{Rb}_{0.5}\text{NO}_3$, $\text{Ca}(\text{NO}_3)_2$ and $\text{C}(\text{NH}_2)_3\text{NO}_3$

Na Du,^{†1} Xintian Wang,^{†1} Ruo Tong Wang,² Enting Xu,¹ Yu Ying Zhu,² Yan Zhao,¹ Peng Ren,^{*1} Fei Yen^{*1}

¹School of Science, Harbin Institute of Technology, Shenzhen, University Town, Shenzhen, Guangdong 518055, P. R. China.

²School of Mechanical Engineering and Automation, Harbin Institute of Technology, Shenzhen, University Town, Shenzhen, Guangdong 518055, P. R. China.

Correspondence: fyen at hit.edu.cn; renpeng at hit.edu.cn.

Abstract: Long-range magnetic ordering of the orbital motion of oxygen atoms within NO_3^- cations is identified from experimental measurements of the magnetic susceptibility $\chi(T)$ in LiNO_3 , $\text{Ca}(\text{NO}_3)_2$, $\text{K}_{0.5}\text{Rb}_{0.5}\text{NO}_3$ and $\text{C}(\text{NH}_2)_3\text{NO}_3$ at their respective order-disorder, solid-solid phase transitions T_N . The observed sharp changes in $\chi(T)$ and accompanying hysteretic behavior indicate the phase transitions to be first order. A model employing the law of conservation of angular momentum is used to explain why the librations between neighboring NO_3^- become geared below T_N . Since the periodic motions involve concerted motion of net charges, the associated magnetic moments of the NO_3^- ions indirectly establish an antiferromagnetic structure below T_N . Our findings identify a previously unidentified type of molecular interaction which may be exploited to further increase the enthalpy of the widely-popular hydrated salts employed as energy storage devices.

Keywords: Angular momentum, magnetism, nitrate salts, order-disorder phenomena, phase transition.

1. Introduction

When a substance undergoes a first-order phase transition, energy is absorbed/released in the latent heat of transition. If the latent heat can be stored and later retrieved and consumed, then the substance may be designated as a “phase change material” (PCM). The practicality of PCMs chiefly depends on the amount of heat absorbed/released in the intended operating temperature range and its transition temperature among many other factors [1-3]. Microscopically, the amount of latent heat across a phase transition is largely dependent on the change in entropy of the material according to how much the individual ions become ordered or disordered. At solid-liquid and solid-solid phase transitions the ordering is usually translational and orientational, respectively. Often in solid-solid phase transitions of salts containing polyatomic ions, the change in entropy is anomalously higher than the expected amount according to all the accountable orientational configurations [4-6]. Recently, we identified that such excess changes in entropy may be due to a previously unaccounted contribution stemming from temporal ordering of the ionic reorientations which also happens to exhibit magnetic behavior [7].

In the case of nitrate salts, the changes in entropy at some of the phase transitions are anomalously larger than their counterpart halide salts [8,9]. The change in entropy ΔS spreads over across the phase transition so the enthalpy values near room temperature are rather large making the series of nitrate salts popular candidates for energy storage applications [1-3,10-12]. Simply accounting for the ordering of the spatial orientations of the nitrate anions NO_3^- does not seem to be sufficient because ΔS is larger than $R \ln 2$ (where R is the natural gas constant) at the solid-solid phase transitions [6,13] so we hypothesized that temporal ordering is also involved. Given the planar nature and symmetry of the nitrate anion, they can easily reorient within their planes with little disturbance to the lattice [14,15]. Even at liquid helium temperatures, the in-plane libration frequencies of many nitrate salts vary from 15 to 32 cm^{-1} [16]. Hence, we picture that at high temperatures, each anion librates independently with respect to its adjacent anions, *i.e.* it randomly rotates back and forth within its plane by

discrete angles of $\pm q$ confined by a wide potential barrier. However, below a threshold temperature T_N , usually the order-disorder phase transition point, the librations become geared with respect to each other so if an NO_3^- rotates by $+q$, then its adjacent neighbors do so by $-q$. Accounting of this temporal ordering mechanism can explain the excess changes in entropy across the solid-solid phase transitions. Incidentally, as an NO_3^- rotates by q , an extremely weak magnetic field is generated which we can approximately equate it to a dipolar magnetic moment μ . If the network of NO_3^- below T_N indeed becomes geared, then an antiferromagnetic structure of μ should emerge (Fig. 1). Macroscopically, antiferromagnetic ordering of negatively charged species causes the magnetic susceptibility to exhibit a pronounced change at the transition temperature. In the cases when all electrons are paired so the system is non-magnetic (diamagnetic), a detection of a sharp change in the magnetic susceptibility at the order-disorder phase transition of a nitrate salt would provide direct evidence of an onset of NO_3^- - NO_3^- magnetic interactions.

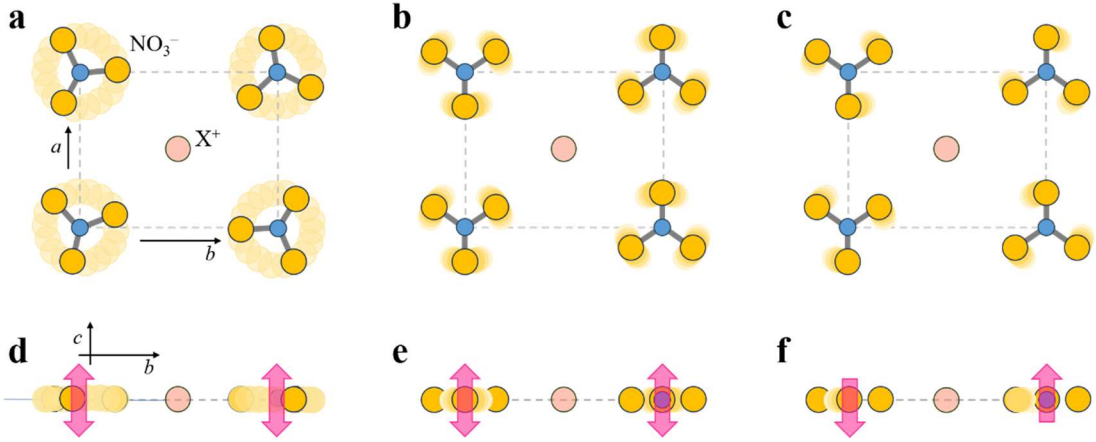


Fig. 1. Schematic diagram depicting the motions and degree of ordering of planar NO_3^- ions along the ab -planes (upper panels) when (a) disordered; (b) orientationally ordered; and (c) temporal ordered. The bottom panels (d)–(f) show associated magnetic moments μ generated by orbital motion of $\text{O}^{2/3-}$ ions. The current consensus is that the system experiences the process from (a) to (b) and (d) to (e) during a disordering-ordering process. In contrast, we suggest the system undergoes the process from (a) to (c) and (d) to (f).

In the following, we report on the experimental measurements of the magnetic susceptibilities as functions of temperature of the diamagnetic salts LiNO_3 , $\text{Ca}(\text{NO}_3)_2$, $\text{K}_{0.5}\text{Rb}_{0.5}\text{NO}_3$ and $\text{C}(\text{NH}_2)_3\text{NO}_3$; they represent nitrate salts with cations that are

spherical univalent/divalent, mixed and polyatomic. We then provide a simple model explaining why temporal ordering of the NO_3^- librations occurs at the phase transitions and how this process, as an indirect consequence, induces antiferromagnetic ordering at the molecular scale.

2. Materials and methods

Anhydrous lithium nitrate LiNO_3 was purchased from Energy Chemicals, Inc. The samples (tiny crystals crushed into powder and pressed into disc pellets) were first annealed at 390 K for 2 hours to remove any remaining H_2O prior to each measurement. Calcium nitrate $\text{Ca}(\text{NO}_3)_2$ was obtained by reacting nitric acid with calcium carbonate. The samples were re-crystallized three times, crushed into powder and pressed into pellets for the measurements. The samples were also annealed at 390 K before the measurements to remove the tetrahydrate phase. Mixed potassium rubidium nitrate $\text{K}_{0.5}\text{Rb}_{0.5}\text{NO}_3$ samples were obtained by mixing an equimolar ratio of KNO_3 and RbNO_3 in deionized H_2O to form a solution and allowed to slowly evaporate at room temperature. The ratio was confirmed by the additivity rule of the molar magnetic susceptibility method [17]. Guanidinium nitrate crystals were grown from the slow evaporation of a solution comprised of its reagent and deionized H_2O . To show the high purity of the samples and the absence of paramagnetic impurities, the expected and experimentally obtained diamagnetic susceptibilities are compared in the Supplementary Material file. The magnetic susceptibility measurements were carried out with the VSM option of a PPMS (Physical Property Measurement System) manufactured by Quantum Design, Inc. The raw data of all the figures along with a more detailed explanation of the experimental procedure is available in the Supplementary Material file.

3. Results and discussion

3.1 Lithium nitrate LiNO_3

Lithium nitrate LiNO_3 is the simplest nitrate salt; its structure remains trigonal from room temperature up to its melting point [18]. According to electrical resistance

measurements a transition occurs at 263 K [19]. Figure 2 shows the molar magnetic susceptibility with respect to temperature $\chi(T)$ of polycrystalline LiNO_3 under an applied magnetic field of $H = 1$ T. The experimentally obtained value of $\chi(300 \text{ K})$ was $-19.5 \times 10^{-6} \text{ cm}^3/\text{mol}$, which is in good agreement with the expected value of $-19.9 \times 10^{-6} \text{ cm}^3/\text{mol}$ according to addition of Pascal's constants [20]. At 264.7 K, $\chi(T)$ increased in magnitude to $-24.7 \times 10^{-6} \text{ cm}^3/\text{mol}$ (by $\sim 27\%$). Upon warming, the phase transition occurred at 302.7 K and $\chi(T)$ reverted back to nearly its original value. Such a drastic change in $\chi(T)$ and a presence of hysteresis can only signify a first-order phase transition involving the ordering of magnetic moments. In the case of negatively charged species, if the change in slope in $\chi(T)$ is positive then the ordering is antiferromagnetic. Since the electrons are paired in LiNO_3 (as it is diamagnetic), the pronounced changes in the measured $\chi(T)$ curves of LiNO_3 is solid evidence of antiferromagnetic ordering of the NO_3^- species.

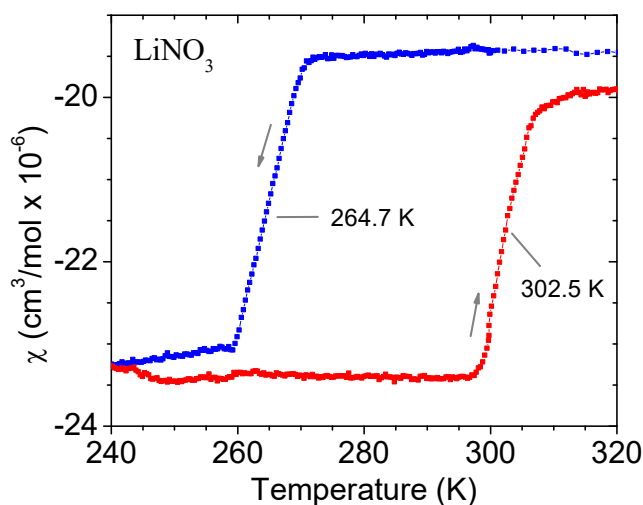


Fig. 2. Molar magnetic susceptibility as a function of temperature $\chi(T)$ of polycrystalline lithium nitrate LiNO_3 under applied magnetic field of $H = 1$ T. Arrows indicate the cooling and warming curves under sweeping rate of 0.5 K/min. Data in all of the figures are available in the Supplementary Material file.

3.2 Calcium nitrate $\text{Ca}(\text{NO}_3)_2$

Calcium nitrate $\text{Ca}(\text{NO}_3)_2$ exhibits a wide λ -peak anomaly in its heat capacity in the range between 280 K and 292 K (with its peak at 287.8 K) [21,22]. Experiments from dielectric constant measurements concurred on the presence of such a solid-solid phase transition just below room temperature [23]. The crystal structure of the room

temperature phase of $\text{Ca}(\text{NO}_3)_2$ is cubic [22] but that of the low temperature phase remains unknown. Given that the NO_3^- of most divalent nitrate salts also exhibit in-plane librations at low temperatures [16], it was natural for us to investigate whether such order-disorder phase transition pertains to an onset-offset gearing of the NO_3^- . Figure 3 shows $\chi(T)$ of polycrystalline $\text{Ca}(\text{NO}_3)_2$. The most remarkable feature is the large hysteretic region in between 245 and 318 K suggesting the phase transition to be first order. However, the region from 289 K to 241 K during cooling (and 293 K to 318 K during warming), where the slope of $\chi(T)$ is positive and continuously changes by over 14% in value, also indicates the phase transition to occur gradually similar to NaNO_3 [24]. A possible mechanism underlying the current case is the occurrence of an intermediate phase where the gearing (or interlocking) of the NO_3^- librations require a finite amount of time to complete. We note that most alkaline nitrate salts exhibit order-disorder phase transitions, but their transition temperatures are much higher than 400 K, the upper limit of our measurement system, so we encourage researchers to investigate their magnetic properties as this should bring forth more information regarding the lattice dynamics of the system.

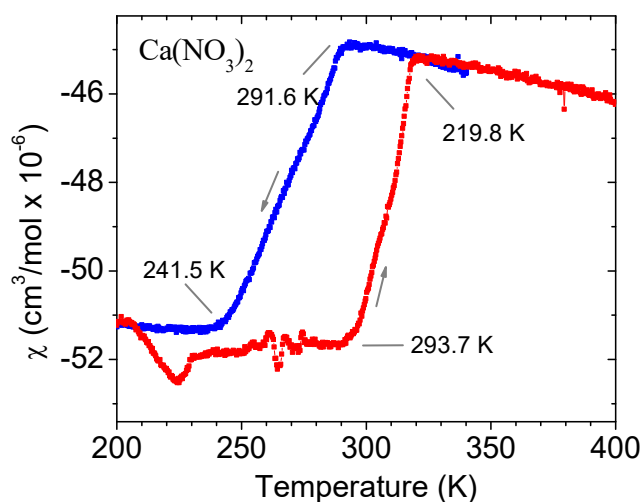


Fig. 3. $\chi(T)$ of calcium nitrate $\text{Ca}(\text{NO}_3)_2$ in polycrystalline form; sweeping rate was 1 K/min.

3.3 Potassium nitrate KNO_3

Potassium nitrate KNO_3 exhibits a phase transition near 402 K when warming from its room temperature ordered phase II to the high temperature disordered phase I.

During cooling, a metastable ferroelectric phase III exists in the region 397–387 K before the system transforms back to phase II [25,26]. With a 50% substitution of K^+ by Rb^+ , the phase transition temperatures II–I, I–III and III–II decrease to around 387, 365 and 355 K, respectively [27,28]. We investigated $K_{0.5}Rb_{0.5}NO_3$ because all of the transition points occur below 400 K. Figure 4 shows $\chi(T)$ of single crystalline $K_{0.5}Rb_{0.5}NO_3$ measured along the 001 direction which is also that of the spontaneous polarization. A rather sharp change of 8.3% occurred in the span of 384.5 ± 1.6 K upon heating indicating the II-I phase transition taking place. During cooling, a similar step-like feature was also observed, but the I-II phase transition seemed to have been interrupted by a presence of a metastable state starting at 376.8 K which can only be attributed to the ferroelectric III phase. Only near 370.0 K did the system seem to have reverted back to phase II. If there were no changes in the magnetic interactions between NO_3^- ions, then $\chi(T)$ would remain independent of temperature; this is true even upon crossing any structural phase transition involving no magnetic ordering. Hence, it is evident that there is also an intimate connection between the ferroelectricity of phase III and the dynamics of NO_3^- ions. Most other univalent nitrate salts such as Na^+ , Rb^+ , Cs^+ , Tl^+ and Ag^+ exhibit solid-solid, order-disorder phase transitions at high temperatures so it is pertinent to investigate their $\chi(T)$ up to their respective melting points in the attempts of better understand their lattice dynamics.

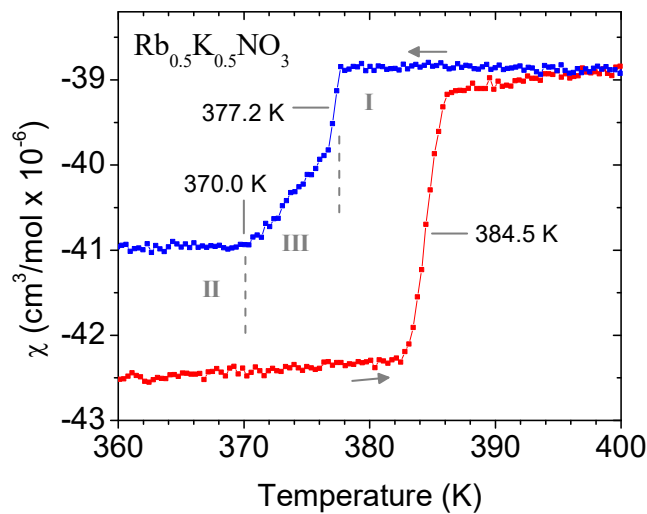


Fig. 4. $\chi(T)$ of potassium rubidium nitrate $K_{0.5}Rb_{0.5}NO_3$ in single crystalline form. $\chi(T)$ and H were along the 001 direction of the crystal and the sweeping rate was 1 K/min.

3.4 Guanidinium nitrate $C(NH_2)_3NO_3$

The order-disorder phase transition of guanidinium nitrate $C(NH_2)_3NO_3$ has been well-studied as it involves an extremely large change of its lattice constant despite the low temperature and high temperature phases remaining monoclinic [29,30]. Existing literature from various types of measurements pinpoint the phase transition to occur at 276 K and 296 K during cooling and warming, respectively [31]. Figure 5 displays $\chi(T)$ of guanidinium nitrate along the 010 orientation of a single crystalline sample. During the first cooling run, no pronounced anomaly was observed. Upon warming, a sharp increase by 9.4% in $\chi(T)$ occurred at 296.4 K. The second cooling run showed a sharp decrease in $\chi(T)$ at 276.3 K. All subsequent runs exhibited pronounced changes near the same transition points but systematically decreasing in magnitude. This can be explained by the fact that the crystals were grown at 295 K so it seems that the NO_3^- were in an ordered state at the start of the experiments. Then, with each cycle the crystal cracked more each time the phase transition was crossed which decreased the number of NO_3^- - NO_3^- interactions.

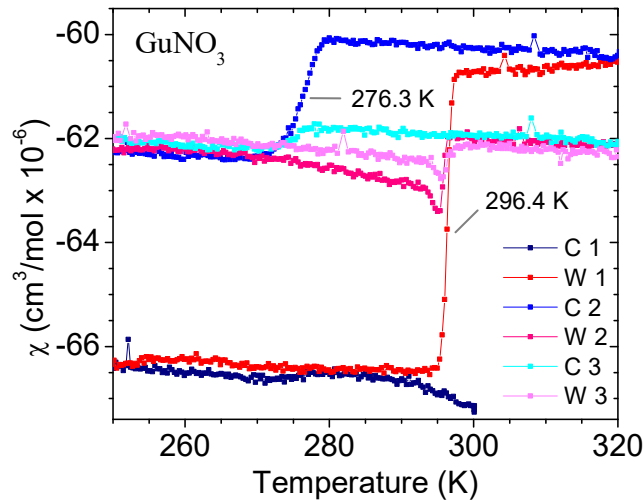


Fig. 5. $\chi(T)$ along the 010 orientation of a guanidinium nitrate crystal measured under 1 K/min.

3.5 Discussion

To explain the reason why an order-disorder phase transition takes place, we make use of the law of conservation of angular momentum. Mathematically, this is expressed

as the total angular momentum $\mathbf{L}_{\text{system}}$ of a closed system remaining constant with respect to time:

$$\frac{d}{dt}(\mathbf{L}_{\text{system}}) = 0$$

In crystalline solids with polyatomic ions, apart from phonons [32,33] $v_n(T)$ contributing to $\mathbf{L}_{\text{system}}$ (where $n = 1, 2, \dots$), the orbital motion of the non-spherical ions also contributes an $m\mathbf{v}_n\mathbf{r}$ component, where m and \mathbf{v}_n are, respectively, the mass and velocity of the non-stationary atoms and \mathbf{r} the average radius of the orbits. For the case of NO_3^- , m would be the masses of the three oxygen atoms, \mathbf{r} the average distance between the O and N atoms and \mathbf{v}_n the speed of the O atoms when the entire anion rotates by an angle q . Since \mathbf{r} , \mathbf{v}_n and v_n are all dependent on temperature T , Eq. 1 can be expanded to become:

$$\frac{d}{dt}(m\mathbf{v}_1\mathbf{r}(T) + m\mathbf{v}_2\mathbf{r}(T) + \dots + v_1(T) + v_2(T) + \dots) = 0$$

We can start by only considering two NO_3^- (mediated by a rigid cation) in the ground state where $m\mathbf{v}_n\mathbf{r} \gg v_n$ (minimal phonon contribution). Hence, from Eq. 2, $m\mathbf{v}_1\mathbf{r} \approx -m\mathbf{v}_2\mathbf{r}$, meaning that if one NO_3^- rotates by q , then the other NO_3^- must rotate by $-q$, *i.e.* the two cations are geared, or “ordered”. As T is increased, the phonon contribution becomes significantly enough that adjacent NO_3^- no longer need to remain geared because there are other channels to conserve angular momentum. Since the oxygen atoms (with negative net charges) at the extremities trace out current loops, each rotating NO_3^- carries with itself an equivalent magnetic moment $\boldsymbol{\mu}$ [34-36]. Hence, $\boldsymbol{\mu}$ is arranged antiferromagnetically in the ordered phase while behaving paramagnetically in the disordered phase. The experimentally measured macroscopic magnetization is sensitive to changes of all of the individual $\boldsymbol{\mu}$ but not v_n . This explains the sharp changes observed in $\chi(T)$ at the order-disorder phase transitions for the present cases of LiNO_3 , $\text{Ca}(\text{NO}_3)_2$, $\text{K}_{0.5}\text{Rb}_{0.5}\text{NO}_3$ and $\text{C}(\text{NH}_2)_3\text{NO}_3$.

4. Conclusions

To conclude, we investigated the magnetic properties of several nitrate salts and found evidence of antiferromagnetic ordering of the magnetic moments arising from

librating NO_3^- . We suggest the formation of the antiferromagnetic structures to be indirect manifestations of the NO_3^- rotors becoming geared due to coarse graining of conservation of angular momentum. Our findings provide an explanation to the excess change in entropy encountered in most nitrate salts as originating from previously not accounting the gearing mechanism of the NO_3^- . Consequently, it is worthy to investigate whether *partial* isotope exchange of the ^{16}O atoms by ^{18}O would increase the magnetic entropy of a system which in turn may *further* increase their heat capacities, thus the enthalpies and energy storage capacities of the currently widely-employed hydrated salts as phase change materials. Lastly, the NO_3^- in divalent nitrates and CO_3^{2-} in carbonates also librate at liquid helium temperatures [16], so we also expect to observe magnetic ordering based on oxygen atom orbitals at the solid-solid phase transitions present in many organic & inorganic nitrates, carbonates and other salts possessing oxyanions.

CRedit authorship contributions statement

Na Du prepared the LiNO_3 samples, grew the $\text{K}_{0.5}\text{Rb}_{0.5}\text{NO}_3$ crystals, performed most of the magnetic susceptibility measurements, and drew Figures 2-6. **Xin Tian Wang** performed XRD analysis on all of the samples. **Ruo Tong Wang** assisted with the magnetic susceptibility measurements, data analysis and plotting of the graphs. **En Ting Xu** grew the guanidinium nitrate crystals and helped synthesize calcium nitrate. **Yu Ying Zhu** and **Yan Zhao** assisted with the magnetic susceptibility measurements, crystal growth process and drawings. **Peng Ren** partly supervised the preparation and quality of the samples. **Fei Yen** designed the project, supervised the experiments and drafted the manuscript.

Data Availability

All data are included in the Supplementary Information file.

Declaration of Competing Interest:

The authors declare no competing financial interests.

References:

1. K. Matuszek, R. Vijayaraghavan, M. Kar, D.R. MacFarlane, Role of hydrogen bonding in phase change materials, *Cryst. Growth Des.* **20** (2020) 1285–1291.
2. S. Ahmed, D. Ibbotson, C. Somodi, P.J. Shamberger, Zinc nitrate hexahydrate pseudobinary eutectics for near-room-temperature thermal energy storage, *ACS Appl. Eng. Mater.* **2** (2024) 530–541.
3. Q. Wang, C. Wu, X. Wang, S. Sun, D. Cui, S. Pan, H. Sheng, A review of eutectic salts as phase change energy storage materials in the context of concentrated solar power, *Int. J. Heat Mass Transfer.* **205** (2023) 123904.
4. S.S. Chang, E.F. Westrum, Jr, Heat capacities and thermodynamic properties of globular molecules. II. Triethylenediamine1, *J. Chem. Phys.* **64** (1960) 1547–1552.
5. J.C. Trowbridge, E.F. Westrum, Jr, Heat capacities and thermodynamic properties of globular molecules. VII. Transition and fusion of Triethylenediamine1, *J. Chem. Phys.* **67** (1963) 2381–2385.
6. D.M. News, L.A.K. Staveley, The significance of entropies of transition in salts, with special reference to nitrates, *Chem. Rev.* **66** (1966) 267–278.
7. M.M. Zhao, N. Du, Y.Y. Zhu, F. Yen, Magnetically driven molecular orientational ordering in plastic crystals: The case of *d*-camphor, *J. Chem. Phys.* **160** (2024) 154506.
8. J.H. Fermor, A. Kjekshus, Entropies and melting points of univalent nitrates, *Acta Chem. Scand.* **24** (1970) 1015–1024.
9. S. Steinert, W. Voigt, R. Glausch, M. Neuschütz, Thermal characteristics of solid–solid phase transitions in long-chain dialkyl ammonium salts, *Thermochim. Acta* **435** (2005) 28–33.
10. E.K. Kouassi, M.W. Manouan, E. Zoro, D. Boa, P. Benigni, H. Zamali, J. Rogez, D. Hellali, Experimental investigation and thermodynamic evaluation of the CsNO₃-LiNO₃-NaNO₃ ternary system, *J. Alloy. Comp.* **864** (2020) 158131.
11. S. Ahmed, A. Hoe, F. Alamo, N. Turner, P.J. Shamberger, Experimental determination of high energy density lithium nitrate hydrate eutectics, *J. Energy Storage.* **52** (2022) 104754.
12. P. Dixit, V.J. Reddy, S. Parvate, A. Balwani, J. Singh, T.K. Maiti, A. Dasari, S. Chattopadhyay, Salt hydrate phase change materials: Current state of the art and the road ahead, *J. Energy Storage.* **51** (2022) 104360.
13. R.W. Carling, Heat capacities of NaNO₃ and KNO₃ from 350 to 800 K, *Thermochim. Acta.* **60** (1983) 265–275.
14. V.M. Trejos, M. de Lucas, C. Vega, S. Blazquez, F. Gámez, Further Extension of the Madrid-2019 Force Field: Parametrization of Nitrate (NO₃⁻) and Ammonium (NH₄⁺) Ions, *J. Chem. Phys.* **159** (2023) 224501.
15. D. Schaefer, M. Kohns, H. Hasse, Molecular Modeling and Simulation of Aqueous Solutions of Alkali Nitrates, *J. Chem. Phys.* **158** (2023) 134508.

16. R.A. Schroeder, C.E. Weir, E.R. Lippincott, Lattice frequencies and rotational barriers for inorganic carbonates and nitrates from low temperature infrared spectroscopy, *J. Res. Natl. Bur. Stand. A Phys. Chem.* **66A** (1962) 407–434.
17. M.M. Zhao, Y. Yang, N. Du, Y.Y. Zhu, P. Ren, F. Yen, Determining the chemical composition of diamagnetic mixed solids via measurements of their magnetic susceptibility, *J. Mater. Chem. C.* **12** (2024) 5877–5885.
18. R. Benages-Vilau, T. Calvet, M.A. Cuevas-Diarte, Polymorphism, crystal growth, crystal morphology and solid-state miscibility of alkali nitrates, *Cryst. Rev.* **20** (2013) 25–35.
19. J.H. Fermor, A. Kjekshus, On the electrical properties of LiNO_3 , *Acta Chem. Scand.* **23** (1969) 1581–1587.
20. G.A. Bain, J.F. Berry, Diamagnetic corrections and Pascal's Constants, *J. Chem. Edu.* **85** (2008) 532–536.
21. C.H. Shomate, K.K. Kelley, The specific heats at low temperatures of nitrates of magnesium, calcium, barium and aluminum, *J. Amer. Chem. Soc.* **66** (1944) 1490–1492.
22. D. Sergeev, B.H. Reis, M. Ziegner, I. Roslyakova, M. to Baben, K. Hack, M. Muller, Comprehensive analysis of thermodynamic properties of calcium nitrate, *J. Chem. Thermodynamics.* **134** (2019) 187–194.
23. D. Bernanrd, Transition de phase dans le nitrate de calcium $\text{Ca}(\text{NO}_3)_2$, *Solid State Comm.* **41** (1982) 79–81.
24. F.C. Kracek, Gradual transition in sodium nitrate. I. Physico-chemical criteria of the transition, *J. Amer. Chem. Soc.* **53** (1931) 2609–2624.
25. F.C. Kracek, The polymorphism of potassium nitrate, *J. Phys. Chem.* **34** (2002) 225–247.
26. S. Sawada, S. Nomura, S. Fujii, Ferroelectricity in the Phase III of KNO_3 , *J. Phys. Soc. Japan.* **13** (1958) 1549.
27. U. Kawabe, T. Yanagi, S. Sawada, Dielectric and x-ray studies of KNO_3 -series mixed crystals, *J. Phys. Soc. Japan.* **20** (1965) 2059–2073.
28. H. Jendoubi, D. Hellali, H. Zamali, M. Jemal, The phase diagram of KNO_3 - RbNO_3 , *J. Therm. Anal. Calorim.* **111** (2013) 877–883.
29. A. Katrusiak, M. Szafranski, Structural phase transitions in guanidinium nitrate, *J. Mol. Struct.* **378** (1996) 205–223.
30. D.P. Karothu, R. Ferreira, G. Dushaq, E. Ahmed, L. Catalano, J.M. Halabi, Z. Alhaddad, I. Tahir, L. Li, S. Mohamed, M. Rasras, P. Naumov, Exceptionally high work density of a ferroelectric dynamic organic crystal around room temperature, *Nature Comm.* **13** (2022) 2823.
31. M. Szafranski, Unusually strong deformation of guanidinium nitrate crystal at the solid-solid phase transition, *Solid State Comm.* **84** (1992) 1051–1054.
32. L.F. Zhang and Q. Niu, Angular momentum of phonons and the Einstein–de Haas effect, *Phys. Rev. Lett.* **112** (2014) 085503.
33. S.R. Tauchert, M. Volkov, D. Ehberger, D. Kazenwadel, M. Evers, H. Lange, A. Donges, A. Book, W. Kreuzpaintner, U. Nowak, P. Baum, Polarized phonons carry angular momentum in ultrafast demagnetization, *Nature.* **602** (2022) 73–77.

34. F. Yen, Z. Zhao, S. Hu, L. Chen, Molecular dynamics of hexamethylbenzene at low temperatures: Evidence of unconventional magnetism based on rotational motion of protons, *Angew. Chem. Int. Ed.* **56** (2017) 13675–13678.
35. F. Yen, L. Meng, T. Gao, S. Hu, Magnetic ordering of ammonium cations in NH_4I , NH_4Br , NH_4Cl , *J. Phys. Chem. C.* **123** (2019) 23655–23660.
36. C.X. Peng, L. Meng, Y.Y. Xu, T.T. Xing, M.M. Zhao, P. Ren, F. Yen, Ferroelectricity driven by orbital resonance of protons in $\text{CH}_3\text{NH}_3\text{Cl}$ and $\text{CH}_3\text{NH}_3\text{Br}$, *J. Mater. Chem. C.* **10** (2022) 1334–1338.